Ionospheric Electron Density During Solar Eclipse of 20 July 1963

by

J. R. Cornellier

T. R. Pound

GP-411

NSG 24

Sponsored by:

National Science Foundation

and

National Aeronautics and Space Administration

Electrical Engineering Research Laboratory

Engineering Experiment Station

University of Illinois

Urbana, Illinois

Ionospheric Electron Density During Solar Eclipse of 20 July 1963

by

J. R. Cornellier

T. R. Pound

GP-411

NSG 24

Sponsored by:

National Science Foundation

and

National Aeronautics and Space Administration

Electrical Engineering Research Laboratory

Engineering Experiment Station

University of Illinois

Urbana, Illinois

Acknowledgement

This work was supported by National Science Foundation Grant GP-411 and National Aeronautics and Space Administration Grant NSG-24. Ionograms were provided by the World Data Center, and the scaled virtual height data were processed by the Institute for Telecommunications Sciences and Aeronomy.

Table of Contents

List of Tables

List of Figures

1. Introduction

The solar eclipse of 20 July 1963 was visible at ground level throughout the North American continent, as well as the northern polar cap and portions of the Atlantic and Pacific Oceans and of South America. The path of total eclipse, again at ground level, crossed North America diagonally, passing just north of Anchorage, Alaska, and continuing southeast through Canada and across the Maine-Canada border. The semi-duration was more than one hour at all points of interest in this study.

Data were obtained during the eclipse at many of the ionosonde stations in the United States and Canada. From among these records those of five stations have been selected for analysis, namely Anchorage, Alaska; Winnipeg and Fort Churchill, Manitoba; Millstone Hill (Westford), Massachusetts; Fort Monmouth, New Jersey. Table 1 lists pertinent geographical and ground level eclipse data at each of these stations. Specific solar obscuration data at heights above ground level are contained in figures 1 through 3 for Millstone Hill, Fort Monmouth, and Anchorage, and in table 2 for the remaining two stations. It should be noted that at two of the locations, Anchorage and Millstone Hill, the eclipse was total at heights of 150-200 and 300 kilometers respectively.

The starting point for this analysis is true height data, N(h), for the daylight hours of 19 and 20 July 1963, derived from the ionograms of the ionosonde stations noted above. Since the range of the electron density profiles spans the height intervals associated by convention with the E, F1, and F2 regions of the ionosphere, it will be convenient to discuss the data according to these height intervals, prefaced by general considerations of the corresponding ionospheric regions.

Table 1. Geographical and Ground Level Eclipse Data

Station	Anchorage Alaska	Ft. Churchill Manitoba	Ft. Monmouth New Jersey	Millstone Hill Massachusetts	Winnipeg Manitoba
Geographic Coordinates	61.2°N 150.0°W	58.8°N 94.2°W	40.3°N 74.0°W	42.6°N 71.5°W	49.9°N 97.4°W
Dip	74.1°	83.5°	71.6°	73.2°	77.7°
Declination	27°E	3°E	10°W	14°W	10°E
First Contact	0850 AST	1352 CST	1544 EST	1540 EST	1400 CST
Middle of Eclipse	1003 AST	1503 CST	1648 EST	1644 EST	1514 CST
Last Contact	1116 AST	1614 CST	1752 EST	1748 EST	1628 CST
Semi-duration	1h 13m	1h 11m	1h 04m	1h 04m	1h 14m
Maximum Obscuration	99.9%	91.3%	91.8%	93.5%	91.8%

Table 2. Eclipse Data Above Ground Level

Station	Height above ground (km)	Maximum solar obscuration (%)	Time of maximum obscuration (CST)	Time of first contact (CST)	Time of last contact (CST)
Winnipeg Manitoba	100	85	1516	1400	1628
	200	87	1516	1400	1630
	300	89	1518	1400	1630
	450	93	1518	1400	1632
Ft. Churchill Manitoba	100	92	1506	1352	1611
	200	90	1506	1351	1614
	300	87	1506	1351	1616
	450	83	1506	1351	1616

Our purpose is to present the true height data for the eclipse period, to note the similarities and dissimilarities in the observations at the different stations, and to investigate the probable causes of the observed behavior with reference to processes occurring in the ionosphere. An initial section reviews the electron density continuity equation and the final section before the conclusions discusses the interpretation of the parameter S_{cat} which is related to the thickness of the F2 peak.

2. The Continuity Equation

The continuity of the electron density at any height is expressed in general form by the equation

$$\frac{\partial N}{\partial t} = q - \begin{matrix}\text{Loss by}\\ \text{Chemical}\\ \text{Processes}\end{matrix} - \begin{matrix}\text{Loss by}\\ \text{Transport}\\ \text{Processes}\end{matrix} \qquad (2\text{-}1)$$

where

q = electron production rate per unit volume

N = electron number density.

The transport term represents a loss (or a gain with the opposite sign) of electrons, since the equation is written on a per volume basis.

The Chapman theory of ionized layers leads to an approximate solution of the continuity equation which has proven useful in regard to ionospheric regions in photochemical equilibrium. Accordingly, it is relevant to review the assumptions which underlie and the equations which describe the Chapman model. The assumptions are the following:

(1) a flat earth,

(2) constant acceleration of gravity, g,

(3) isothermal atmosphere composed of a single ionizable species, distributed exponentially, that is

$$n(h) = n_o \exp(-h/H) \qquad (2\text{-}2)$$

where

$n(h)$ = number density of the ionizable species,

H = scale height = constant,

k = Boltzmann's constant,

T = absolute temperature,

m = mass of the ionizable species,

(4) monochromatic radiation, I, incident at an angle χ with the earth's normal,

(5) rate of ion-electron pair production equal to the rate of absorption of the radiation.

The relations follow immediately from the assumptions. First the rate of radiation absorption is

$$\frac{d}{dh} I(h) = \sigma \sec \chi \; I(h) \; n(h) \tag{2-3}$$

where σ, the cross-section for absorption, is interpreted as the probability that a photon will be absorbed in unit time if there is unit incident radiation flux. Integration and application of the upper boundary condition

$$I(h = \text{top of atmosphere}) = I_\infty \tag{2-4}$$

yield

$$I(h) = I_\infty \exp \left[-\sigma \sec \chi \int_h^\infty n(h') \, dh'\right] . \tag{2-5}$$

Assumption (3) permits evaluation of the remaining integral which leads to

$$I(h) = I_\infty e^{-\tau} \tag{2-6}$$

where

$$\tau = \text{optical depth} = \sigma \sec \chi \; n(h) \; H . \tag{2-7}$$

Assumption (5) can be expressed mathematically by

$$q(h) = -\frac{dI}{ds} = \cos \chi \frac{dI}{dh} \tag{2-8}$$

and differentiation of equation (2-6) provides an expression which may be substituted for the derivative in equation (2-8) to obtain

$$q(h) = I_\infty \sigma e^{-\tau} n(h) . \tag{2-9}$$

The maximum production rate can be determined in the usual manner and substituted in equation (2-9) yielding

$$q(h) = q_m \exp\left[1 - \frac{h-h_m}{H} - \exp\left(-\frac{h-h_m}{H}\right)\right] \tag{2-10}$$

where

h_m = height of maximum production

$$q_m = q_o \cos \chi \tag{2-11}$$

$$q_o = q(h = h_m \text{ and } \chi = 0) \; . \tag{2-12}$$

The height of maximum production is found, again by the usual method, to be given by

$$\exp(h_m/H) = n_o \sigma H \sec \chi \; . \tag{2-13}$$

The loss processes must also be considered. If it is assumed that

(1) transport process may be neglected,

(2) chemical loss processes other than ion-atom interchange and dissociative recombination, successively, can be neglected, and

(3) there is a single molecular species,

then for a given height

$$\frac{d}{dt} n(A) = q - \beta\, n(A) \tag{2-14}$$

$$\frac{d}{dt} n(M) = \beta\, n(A) - \alpha\, n(M)\, N \tag{2-15}$$

$$\frac{d}{dt} N = q - \alpha\, n(M)\, N \tag{2-16}$$

where

$n(A)$ = atomic ion density

$n(M)$ = molecular ion density

α = dissociative recombination coefficient

β = linear loss coefficient.

Further assumptions that the time derivatives are negligible and that the ionosphere is electrically neutral lead to a simple form of the continuity equation

$$0 = q - \frac{\alpha \beta}{\beta + \alpha N} N^2 \qquad (2\text{-}17)$$

It has been shown (Ratcliffe, 1956b; Hirsh, 1962) that the equation

$$\frac{dN}{dt} = q - \frac{\alpha \beta}{\beta + \alpha N} N^2 \qquad (2\text{-}18)$$

is a very good approximation to equation (2-16) whether or not the time derivatives in equation (2-14), (2-15), and (2-16) vanish.

It should be noted that α, the dissociative recombination coefficient is not height dependent (except possibly through temperature dependence) but that β, the linear loss coefficient, is of the form

$$\beta = \gamma\, n(M) \qquad (2\text{-}19)$$

where γ is the rate coefficient of the ion-atom interchange reaction. Consequently, β is a strong function of height. Equation (2-18) remains valid for an atmosphere with two molecular constituents provided α and β are interpreted as effective coefficients, properly determined from parameters associated with the two constituents. In this case, α and β will both be height dependent (Hirsh, 1962).

If $\beta \gg \alpha$, equation (2-18) can be simplified to

$$\frac{dN}{dt} = q - \alpha N^2 . \qquad (2\text{-}20)$$

If photochemical equilibrium is assumed and the production expression previously derived (equations (2-10) and (2-11)) is substituted for q, equation (2-18) becomes

$$N = \left(\frac{q_o}{\alpha} \cos \chi\right)^{1/2} \exp \frac{1}{2} \left[1 - \frac{h-h_m}{H} - \exp\left(- \frac{h-h_m}{H}\right)\right] \qquad (2\text{-}21)$$

which describes a Chapman α-layer. When this equation is evaluated at the height of maximum electron production, the exponential factor is unity and

$$N_m = \left(\frac{q_o}{\alpha} \cos \chi\right)^{1/2} . \qquad (2\text{-}22)$$

Similarly, if $\alpha \gg \beta$, equation (2-18) reduces to

$$\frac{dN}{dt} = q - \beta N . \qquad (2\text{-}23)$$

When, as before, photochemical equilibrium is assumed and the expression for q in equations (2-10) and (2-11) is substituted, equation (2-18) becomes

$$N = \frac{q_o}{\beta} \cos \chi \exp \left[1 - \frac{h-h_m}{H} - \exp\left(- \frac{h-h_m}{H}\right)\right] \qquad (2\text{-}24)$$

which describes a Chapman β-layer. At the height of maximum electron production,

$$N_m = \frac{q_o}{\beta} \cos \chi . \qquad (2\text{-}25)$$

In practice, the Chapman α-layer is more useful than the β-layer as an approximation to actual ionospheric behavior, because at the higher levels where we expect $\alpha \gg \beta$, transport processes become increasingly significant. The α-layer model finds application primarily in the E and to a lesser extent in the F1 region. At lower levels, i.e., in the D region and the C region, if it is considered distinct from the D region, assumption (2) regarding chemical processes is not well justified.

The effects of transport processes and other departures from the Chapman theory will be considered in the discussions of the individual ionospheric regions that follow.

3. The E Region

The electron density distribution in the lower E region below the turbopause (approximately 110 km) is complicated by mixing processes. Since the true height data presented in this report do not extend down this far, we will limit our discussion to heights above the turbopause.

Proposed production processes in the E region have been summarized by Nicolet (1962) as the ionization of molecular oxygen and molecular nitrogen by x-radiation, of molecular oxygen by UV radiation, and of atomic oxygen by both UV and x-radiation. There is general agreement that the principal loss process is dissociative recombination although the agreement does not extend to the specific chemical reactions involved.

The nature of the chemical processes and the further fact that in this region photochemical equilibrium is established during the daytime suggest that the electron density distribution should be approximately that predicted by the Chapman layer theory, a conclusion that has been confirmed by many observations. Departures from the Chapman model become apparent when the recurring variations in the E region are considered. To minimize these differences, generalizations of the theory have been accomplished, as noted in the standard texts, for the cases of spherical earth, non-isothermal atmosphere, polychromatic radiation, and multiple molecular species.

Results of early eclipse studies have been tabulated by Ratcliffe (1965a). In regard to the E region, these investigations are primarily directed toward obtaining the value of the effective recombination coefficient, α_{eff}. The method most commonly adopted for this purpose is based on the continuity equation, simplified by neglecting transport effects and by considering only the quadratic loss (i.e., equation (2-20)). The product of the Chapman production function and the fraction of the solar disc unobscured

then serves as the production term to complete the model. The value of α_{eff} can be inferred from the variation of N_mE during the course of the eclipse--more specifically from the maximum and minimum observed values of N_mE, the times at which they occurred and the calculated value of the production term for these times. Alternatively, trial values of α_{eff} can be selected and theoretical N_mE versus time curves calculated by means of the ionospheric model. The theoretical curve which best fits the experimental curve then indicates the correct value of α_{eff}.

Although these methods, in addition to the neglect of transport phenomena, are non-rigorous for reasons summarized by Ratcliffe, the results indicated the non-uniform brightness of the solar disc and further indicated the presence of incident radiation during eclipse totality before this fact of coronal radiation was confirmed by direct measurements (Friedman, 1960).

Values of the effective recombination coefficient determined by these methods and later, by more refined techniques (e.g., Minnis, 1956; Szendrei and McElhinny, 1956) agree with few exceptions on an order of magnitude, viz. 10^{-8} $cm^3 sec^{-1}$. Bowhill (1961) subsequently considered a two ion model and determined the values of the two components of α_{eff} considering separately both eclipse data and measurements of f_oE diurnal variations. The conclusions in both bases indicated that the components of α_{eff} are of different orders of magnitude, viz. 10^{-7} and 10^{-9} $cm^3 sec^{-1}$. This result implies a time variation of the effective recombination coefficient, since the larger component would initially predominate but become less significant as the concentration of the related ion decreased.

Data for the 20 July 1963 eclipse are displayed as true height, N(h) profiles in figures 4 through 8. For each station, curves were plotted for the three times corresponding closely to beginning, middle, and end of

eclipse conditions. The graphs show similar E region behavior for the five stations, a decrease in the number density at all heights through the first half of the eclipse period followed by an increase, after maximum eclipse phase. The difference between pre- and post-eclipse values of electron density at fixed heights in the E region is notably different at stations that are geographically far apart and agrees with the normal diurnal variation of the region. Thus at Anchorage where the eclipse occurred in the morning the E region electron density returned to the pre-eclipse value, whereas at the eastern stations where the eclipse occurred in the afternoon the electron density did not return to the pre-eclipse value in the E region. Intermediate stations show intermediate results.

Rocket measurements of electron density above Fort Churchill, Manitoba, during the eclipse (Smith et al., 1964) showed a decrease in E region electron density without appreciable change in the shape of the profile. This observation is in close agreement with the ionosonde data. The rocket measurements further indicated a time lag of less than three minutes between N_mE and maximum eclipse phase which, together with the ionosonde data, implies a minimum value of 1×10^{-7} cm^3 sec^{-1} for the effective recombination coefficient, α_{eff}, in the E region.

4. The F1 Region

Electron production at F1 heights is generally attributed to the ionization of atomic oxygen and molecular nitrogen by solar UV (200-850 Å) and x-radiation, and electron loss to dissociative recombination of molecular oxygen, molecular nitrogen, and nitric oxide. There is considerable doubt as to the predominant ion-atom interchange reaction that precedes the dissociative recombination. It is expected that more reliable determination of the associated rate constants together with more detailed knowledge of the composition of the atmosphere at this level will resolve the ambiguity.

It has long been observed that the critical frequency f_oF1, when it appears on the ionograms, varies approximately as the peak of an idealized Chapman α-layer, but corresponds on the true height curves to a ledge on the electron density profile rather than to a peak, with but few exceptions. The pattern of occurrence of f_oF1 can be summarized as follows:

(1) never at night,

(2) more often at midday, and

(3) preferably at sunspot minimum.

A relatively simple theory to account for the splitting of the F layer has been formulated by Ratcliffe (1956b) and Hirsh (1959) and since summarized elsewhere (e.g., Risbeth, 1962). The ledge which characterizes the F1 region on the true height curves is shown to result if the transition from quadratic to linear loss occurs at the height of maximum electron production. The derivation assumes photochemical equilibrium in addition to those assumptions previously listed for the Chapman production function and the simplified continuity equation, so that

$$0 = q - \frac{\alpha \beta}{\beta + \alpha N} N^2 \qquad (2\text{-}17)$$

with solution

$$N = \frac{q}{2\beta}\left[1 + \left(1 + 4\frac{\beta^2}{\alpha q}\right)^{1/2}\right] . \qquad (4\text{-}1)$$

The shape of the profile in the vicinity of the production peak is governed by

$$r = \beta(\alpha q)^{-1/2} \qquad (4\text{-}2)$$

where the expression on the right is to be evaluated at the height of the production peak. It is found that for $r > 2$, a prominent ledge appears in the electron density profile.

In order to predict the shape of the profile, it is necessary to write the functional dependence of r on q and on χ. Since β is proportional to the concentration of the molecular constituent involved in the ion-atom interchange reaction (equation (2-19)) and since this constituent is distributed exponentially

$$\beta = \beta_m \exp\left[-\frac{h-h_m}{H_m}\right] \qquad (4\text{-}3)$$

where

h_m is the height of the production peak

β_m is the value of β at $h = h_m$

H_m is the scale height of the constituent involved in the ion-atom interchange reaction.

Defining

$$k = H_i/H_m \qquad (4\text{-}4)$$

where H_i is the scale height of the ionizable constituent, the last two equations can be combined to yield

$$\beta = \beta_m \exp\left[-k\frac{h-h_m}{H_i}\right] . \qquad (4\text{-}5)$$

Substituting expressions from equations (4-4), (2-11), and (2-13) in equation (4-2) leads to

$$r(\chi) = \frac{\beta_m (\cos \chi)^{k-1/2}}{(\alpha q_o)^{1/2}} \qquad (4\text{-}6)$$

where

$$q_o = q(h = h_m \text{ and } \chi = 0) \qquad (2\text{-}12)$$

and α is assumed constant.

Taking atomic oxygen as the ionizable constituent, k = 2 if the molecular constituent involved in the ion-atom interchange reaction is molecular oxygen and k = 1.75 if the molecular constituent is nitrogen. Thus the appearance of the F1 ledge toward midday and more often in summer is predicted by the variation of r with χ. Its appearance more often during sunspot minimum periods follows from the inverse variation of r with q_o.

Before discussing eclipse observations relating to the F region, it is prudent to review briefly two problems in the interpretation and reduction of the associated ionograms, the "valley" problem and the possibility of oblique reflections. Both of these problems have been considered by Gledhill (1959) who concluded from computations using a relatively simple model of the ionosphere that the possible error might be significant. Since the error, if any, introduced in the true height data would be most difficult to evaluate precisely, a reasonable limit on detailed conclusions from the data must be recognized.

The "valley" problem occurs whenever the electron density below the F2 peak is not a monotonically increasing function of height. A "valley" may be defined as any height interval below the F2 peak in which the electron density is less than the density at any lower height. It is immediately evident that radio sounding techniques cannot obtain information about the

electron density in the "valley" since the signals will be reflected at the lower height where the electron density is equal to that of the "valley." Since the true height data is normally obtained by assuming that the electron density is a monotonically increasing function of height, although several methods for obtaining more exact profiles have been suggested (e.g., Paul and Wright, 1964), the occurrence of a "valley" would cause the data for heights above the "valley" to be in error to some degree. A "valley" may be formed during an eclipse because the smaller recombination coefficient at the higher levels does not permit the electron density at these levels to react as rapidly as that in the lower regions to changes in production occurring during the eclipse. By this mechanism, a "valley" could be formed above the height of f_oF1, introducing error in the true height data for the F2 peak.

Because the solar obscuration during an eclipse on a surface of constant height is not uniform, horizontal gradients in the electron distribution are introduced. Consequently, there is the possibility of enhanced oblique reflections which can complicate interpretation of ionograms.

A large proportion of F1 region eclipse observations have been concerned with the calculation of the effective recombination coefficient by the same methods as were noted in connection with the E region. Since the calculations have been based on theoretical models which assume only quadratic loss, a high degree of precision could not be expected in results relating to the F1 region, where the effects of linear loss become significant, as we have indicated.

More relevant to our investigation is the tendency of solar eclipses to alter the pattern of occurrence of the F1 ledge, causing it to appear when it would not otherwise have been expected or to disappear when it would have remained according to its diurnal variation. An example, well documented

from the aspect of control data, of the former behavior is the 1961 eclipse over Athens (Ilias and Anastassiadis, 1964). On that occasion, f_oF1 appeared on the ionograms during an early morning eclipse several hours earlier than on the control days which included the entire eclipse month.

Although the appearance of f_oF1 following the onset of an eclipse is consistent with the theory of the F1 region we have outlined, the opposite effect cannot be reasonably explained in terms of this model, which predicts an increase in the parameter r and consequently a better defined F1 ledge for any decrease in electron production. It should be noted that since the theory was developed in terms of static conditions which do not prevail during an eclipse, its use in predicting eclipse phenomena is not justified.

The true height curves for the 20 July 1963 eclipse, figures 4 through 8, all include a well defined F1 ledge at the beginning of the eclipse, a normal situation for daytime in mid-summer, during sunspot minimum. At mid-eclipse, a ledge is barely discernible at Fort Churchill and not at all at Millstone Hill and at Winnipeg. The density profiles for intermediate times, which are not included in this report, indicate that the smoothing of the profile and subsequent return of the ledge is a gradual process as would be expected. The ionograms also show a gradual loss of the initially well defined f_oF1 cusp. The intermediate time profiles further indicate that h_mF1 did not vary appreciably during the eclipse. Post-eclipse conditions are in agreement with the time of day. At Anchorage, the electron density returned approximately to the value at first contact and the characteristic ledge was well defined following the eclipse, whereas at the eastern stations, the post-eclipse electron density is lower and the ledge is not so well defined as at the beginning of the eclipse.

It is clear from the variety of eclipse effects that have been observed that the F1 region cannot be explained entirely in terms of photochemical quasi-equilibrium.

5. The F2 Region

We have previously noted that above the level of maximum production, which is in the F1 region, the electron density increases with height because the rate of loss decreases more rapidly than the rate of production. The increase in electron density does not continue indefinitely but terminates at the F2 peak, where the effects of loss, production, and diffusion approximately balance one another in the daytime. Since the condition of diffusive equilibrium is rapidly attained above the F2 peak, the daytime F2 region in the neighborhood of the peak is the transition between levels of photochemical equilibrium below and diffusive equilibrium above. A corollary is that the ionization at the daytime F2 peak is not entirely in either diffusive or photochemical equilibrium. For sunspot minimum conditions, experimental observations of the electron density around the F2 peak are in fact readily explained in terms of only production and diffusion in this region with electron-ion recombination confined to the region below 200 km (Pound and Yeh, 1965).

Diffusion of the ionization through the neutral atmosphere is properly termed ambipolar diffusion because the electrostatic forces compel the electrons and the ions to migrate together. Accordingly, the height variation of the ionization is characterized by a single scale height which depends on the temperatures of both the ions and the electrons, and on the mass of the ions, since the mass of the electrons is relatively negligible. The scale height with which the ionization is distributed in the diffusive equilibrium region is

$$H_p = \frac{kT_i}{m_i g}\left(1 + \frac{T_e}{T_i}\right) \qquad (5\text{-}1)$$

where

T_e = electron temperature

T_i = ion temperature

m_i = mass of the ions

and H_p = scale height of the ionization.

If the mass of the ions is approximately equal to that of the neutral particles, which is true in the F2 region, and if the ion temperature is approximately equal to the neutral temperature, which is true in the vicinity of the F2 peak, then the scale height of the ionization is related to the neutral scale height by the equation

$$H_p = H_n \left(1 + \frac{T_e}{T_i}\right) . \qquad (5\text{-}2)$$

The variation of the electron and the ion temperature has been the subject of several relatively recent investigations (Hanson, 1963; Dalgarno et al., 1963). We will merely discuss the physical processes that cause the particle temperatures to differ and then indicate the typical variation of T_e and T_i for conditions of low solar activity.

Some of the energy absorbed by the atmosphere in the process of photoionization appears as kinetic energy of the photoelectrons. This energy can be transferred to the neutral particles and to the ions by both elastic and inelastic collisions. However, the mass ratio and the relatively low ion density compared to that of the neutrals lead to the conclusion that the ions are unimportant in thermalizing energetic photoelectrons. Again because of the mass ratio, elastic collisions with neutrals are unimportant, but inelastic collisions between photoelectrons and neutrals are important in thermalizing photoelectrons in the lower ionospheric regions. The photoelectrons can also transfer energy to the ambient, thermal electrons by elastic collisions, and this process is important above the F2 peak. The

last few electron volts of photoelectron energy is put into the ambient electrons. This causes their temperature to rise above the neutral temperature. The ambient electrons are cooled via energy transfer to the ions, but at lower altitudes the ions and neutrals are in sufficiently good thermal contact that the ion temperature is the same as the neutral temperature. However at higher altitudes the ions are not in sufficiently good thermal contact with the neutrals to transfer energy rapidly enough to keep from being raised to the same temperature as the electrons. The temperature differences at any height, that is $(T_i - T_n)$ and $(T_e - T_n)$ depend on the relative importance of all the energy transfer processes.

A recent analysis of the electron and ion temperature variation which included the effect of thermal conductivity in the electron gas (Geisler and Bowhill, 1965) indicates that at sunspot minimum the neutral, ion, and electron temperatures are equal at heights below approximately 160 km. Above this level the temperature difference $(T_e - T_n)$ rises rapidly until T_e is roughly two times T_n, during the daytime. On the other hand, T_i remains approximately equal to T_n until about 300 km. Above this level the difference $(T_i - T_n)$ increases until T_i equals T_e at 1000 km, approximately. Thereafter, T_e and T_i remain equal. These results were shown to compare favorably with experimental data.

The variation of f_oF2 during solar eclipses has been regularly observed, but correlation with other ionospheric parameters or processes has generally been unsuccessful due to the irregular nature of the variations. A correlation between the variation of f_oF2 and the change in electron temperature was suggested by several observations of the 20 July 1963 eclipse based on electron content measurements and ionosonde data (Pound, 1964; Pound et al., 1966) and incoherent backscatter measurements (Evans 1964, 1965a). Following a review of f_oF2 records during this and prior eclipses, Evans

(1965b) summarized the theory in the following two conditions which are necessary for an increase in f_oF2 during a solar eclipse:

(1) Total or nearly total eclipse at F1 region heights,

(2) Magnetic dip $\geq 60^o$.

These conditions follow immediately from the hypothesis that the increase in the critical frequency is the result of a rapid transport of ionization downward from heights above the F2 peak, occasioned by a rapid decrease in the electron temperature, and consequently in the scale height of the ionization. The first condition insures that the electron temperatures will decrease, since the production peak is in the F1 region. The second condition is necessary for sufficient downward diffusion to take place, since charged particles in the ionosphere move only along the lines of the magnetic field.

The two conditions may not be sufficient because the magnitude of f_oF2 is determined by the resultant of production, recombination, and diffusion effects. Therefore, some quantitative measure would be required for predicting an increase in f_oF2 with certainty.

We are not however exclusively interested in the variation of the critical frequency but rather in the electron density distribution through the eclipse period. Since N(h) curves are not convenient to observe the electron density at a sequence of times, graphs of constant electron density have been prepared for three of the stations, viz. Millstone Hill, Fort Monmouth, and Anchorage (figures 9 through 11). The curves are plotted for constant log of the plasma frequency (Mhz). For clarity the stations will be discussed in turn, following preliminary remarks about the solar radiation during the eclipse period.

The Stanford 9.1 cm spectroheliogram for 20 July 1963 shows unusually bright solar areas situated at both the east and the west limbs and a third

such area near the center of the solar disc. Measurements of 915 Mhz solar flux at Bedford, Massachusetts (Miner, 1964) show unusual variations at 1637 and 1657 EST which correlate with the covering of the bright area on the east limb and the uncovering of that on the west limb. This correlation provides specific times for some of the variations in solar radiation that resulted from the non-uniform brightness of the solar disc. The times apply equally to Millstone Hill which is 26 miles from Bedford.

At Millstone Hill (see figure 9), prior to the eclipse, the electron density was increasing at heights above 210 km and decreasing below that level. Since the mid-afternoon time implies decreasing production the increase at the higher levels must be attributed to downward diffusion of the ionization from above the peak, whereas the decrease at the lower levels is due to recombination. The constant density at heights near 210 km indicates that downward diffusion of electrons approximately balanced decreasing production and recombination. Thus, above about 210 km diffusion certainly predominated over loss, while below this level down to about 200 km it is likely that downward diffusion of electrons to the more lossy lower region below 200 km was rapid enough to cause the electron density to decrease.

Following first contact (1542 EST) the electron density decreased at all levels as expected, since transport from above the peak could not immediately counteract the sudden decrease in production. The decrease in electron density was noticeably more rapid near the production peak at approximately 170 km. The decrease of electron density just below the F2 peak shortly gave way to an increase. This change is due to the downward transport of electrons to the region of the peak.

The large variations in electron density between 1550 and 1609 EST indicated by the contours do not seem reasonable. It may be that the 1600

EST data which alone determine the large dip in the contours are in error, since the Millstone Hill ionograms were of poor quality and since the contours for Fort Monmouth do not show this dip, although the graphs are otherwise very similar.

Between 1609 and 1637 EST there was some fluctuation in the electron density at all but the lowest heights. The net effect was an increase in the density above 240 km and a net decrease below this level. The behavior is similar to that prior to the eclipse except that the rate of change is different. The decrease of electron density between 210 and 240 km does not have to be attributed to recombination since it could also be due to the continuing decrease of production and to the transport of electrons from this region down to the more lossy region around 200 km. During this interval, f_oF2 rose steadily which is consistent with a downward flux from above the peak.

Following 1637 EST, the electron density at most heights decreased in response to the covering of an exceptionally bright area on the solar disc. The behavior of the ionization was similar to that at first contact except that the electron density remained constant at the upper heights below the peak. The critical frequency increased slightly, attaining its maximum eclipse value at approximately 1640 EST.

Following 1640 EST the density increased at all levels except near the peak. The increase continued through the period of maximum phase, at 1650 EST at the lower levels. However, a decrease began at the altitudes just below the peak indicating that ionization was being raised to higher altitudes by the increase of the electron temperature during the second half of the eclipse. Following 1645 EST, the uncovering of an unusually bright solar area caused a sudden increase in the electron density at lower heights, but

a decrease at higher levels due to increased production and electron temperature. After 1752 EST a pattern analogous to that after 1620 became evident, i.e., at the same height levels, the opposite effects corresponding to decreasing and increasing eclipse phase appeared at these times. The decreasing electron density at the higher altitudes together with a steady decrease in the critical frequency indicate upward transport dominant down to 200 km approximately, below which the increase in density indicates that production was dominant.

At last contact, 1748 EST, the electron density was lower than at first contact, which is to be expected for a late afternoon eclipse.

The contours of constant plasma frequency at Fort Monmouth (see figure 10) are very similar to those at Millstone Hill except for the interval 1550-1609 EST previously noted. The demarcation between upper regions where transport is dominant and lower regions where the loss is more significant appears to be at a higher altitude than at Millstone Hill and is clearly indicated between 1550 and 1630 EST. The decrease in electron density at heights near the production peak was again very rapid and analogous behavior between the first and second halves of the eclipse are similarly well indicated.

At Anchorage (see figure 11), where the eclipse occurred in the morning, the electron density at all heights of interest was increasing prior to the eclipse. Following first contact at 0848 AST, the expected decrease in electron density occurred at all heights, followed shortly by increasing density at the higher altitudes. The transition between height regions characterized by loss and by transport effects occurred at approximately 200 km.

The peaked contours at 0935 AST could be the result of irregular solar brightness, since the uncovering of an unusually bright area would cause a decrease in the electron density as did occur. However, a similar explanation

cannot be invoked to explain the variation of the electron density at 1015 AST, since this would require the covering of a bright area after maximum eclipse phase. Electron density at last contact was somewhat higher than at first contact, which is normal for a morning eclipse.

In summary, the overall behavior of the electron density distribution at the three stations where this distribution was considered in detail shows many similarities although the pre- and post-eclipse values were different, as they were expected to be.

Excluding brief fluctuations which are believed to result from the covering and uncovering of unusually bright areas on the solar disc and those whose origin is entirely uncertain, the similarities in the pattern of electron density variation can be summarized as follows:

(1) a decrease at all levels following first contact,

(2) a change to increasing electron density beginning at the higher levels and continuing down to an intermediate level around 210 or 240 km,

(3) an increase at almost all levels following maximum eclipse phase, and

(4) a change to decreasing electron density beginning at the highest levels below the F2 peak and extending down to the same level as in (2).

This behavior agrees very well with the theory that downward diffusion caused by decreased electron temperatures causes an increase in f_oF2 during an eclipse, and further indicates the general height intervals where the transport processes dominate. The differences between pre- and post-eclipse electron density values at the different stations agree with the time of day at which the eclipse occurred. Post-eclipse values were higher only at Anchorage where the eclipse occurred in the morning.

6. The Parameter S_{cat}

The parameter S_{cat} is one of several thickness parameters relating to the F2 peak. S_{cat} is defined by means of the parabola

$$N = N_m[1 - (\frac{h-h_m}{Y_m})^2] \tag{6-1}$$

fitted to the underside of the F2 peak. N_m, the peak electron density, and values of the true height curve are used to obtain Y_m after which S_{cat} is obtained from the definition (Wright, 1962)

$$S_{cat} = \frac{1}{2} Y_m . \tag{6-2}$$

The parabola of equation (6-1) closely approximates the peak of a Chapman distribution which is described by

$$N = N_m \exp \frac{1}{2}[1 - \frac{h-h_m}{H} - \exp(- \frac{h-h_m}{H})] \tag{6-3}$$

(Wright, 1962). This fact can readily be verified. Power series approximation of the exponential terms in equation (6-3) yields

$$N = N_m[1 - (\frac{h-h_m}{2H})^2] \tag{6-4}$$

which is the same as equation (6-1) provided

$$\frac{1}{2} Y_m = H . \tag{6-5}$$

The above analysis thus leads to

$$S_{cat} = H . \tag{6-6}$$

The power series approximation required to obtain equation (6-4) from equation (6-3) retains three terms of the series for the inner exponential

and two terms for the remaining exponential factor. These approximations do not introduce error greater than 5.5% if the exponent is less than 0.6 for the three term series and 0.3 for the two term series.

The interest in the relations of equations (6-4) and (6-6) arises from the fact that equation (6-3) is also a theoretical result for a layer where the processes of production and recombination type loss are in equilibrium, although in this case h_m refers to the height of maximum production and not to the height of the F2 peak. It has also been shown that it is the equilibrium form theoretically expected of a layer under the combined influence of diffusion and attachment like loss (Hirono, 1955). Non-equilibrium temperatures can be introduced by the relation

$$S_{cat} = \frac{1}{2} H(1 + \frac{T_e}{T_i}) \qquad (6\text{-}7)$$

(Wright, 1964). It should be noted, however, that the relation between S_{cat} and scale height is valid only for equilibrium conditions for which the profile can be approximated by a Chapman distribution.

To test the validity of this relation, the scale height over Millstone Hill at intervals of roughly a half-hour was computed using T_i, T_e, and (T_e/T_i) as determined by Evans (1965a). These values appear in table 3 together with values of S_{cat} computed from the definition. Agreement is not found at any time. The closest approximation to agreement occurs during the eclipse period although one would expect the best agreement during approximately static periods such as prior to the eclipse.

Values of S_{cat} were plotted versus time for the eclipse day and control days where data were available. The graphs appear in figures 12 through 16. It is immediately evident from the graphs that S_{cat} fluctuates rapidly and might perhaps be more useful in terms of averaged values. At several stations,

Table 3. Comparative Calculation of S_{cat}

Millstone Hill, 20 July 1963:

EST	S_{cat} (km) determined by parabola fitted to true height curve at F2 peak:	S_{cat} (km) calculated from the equation $S_{cat} = \frac{1}{2} H(1 + \frac{T_e}{T_i})$
1429	42.8	76.2
1459	54.7	76.2
1532	48.6	65.7
1600	52.0	45.7
1630	42.7	40.0
1657	42.7	45.7
1730	42.2	45.7
1800	42.7	48.6

the fluctuations were severely reduced during the time of the eclipse. This effect is most evident at Winnipeg where a "bite-out" shape characterizes the graph during the first two hours of the eclipse which lasted approximately two and one half hours at that station. A similar but less pronounced effect occurred at Fort Churchill. At Anchorage the eclipse decreased the parameter values and at Millstone Hill it reduced the variations but not the approximate average value. No effect was evident at Fort Monmouth.

From the above considerations, it seems reasonable to conclude that S_{cat} is not a useful approximation to the scale height above the F2 peak and that the thickness of the peak and consequently the parameters that describe it are related to the electron and ion temperatures in some other manner. However, the results do tend to show that a relaxation of the electron temperature results in a decrease of S_{cat}.

7. Conclusions

The following conclusions follow from the data presented and the discussions relative to the different ionospheric regions:

(1) In the E region, the electron density at all the stations was clearly under close solar control, showing a decrease from first contact to the approximate time of maximum obscuration and thereafter an increase. Post-eclipse values were higher than the pre-eclipse values at Anchorage, and lower at the other stations, the difference being greater at the eastern stations where the eclipse occurred late in the afternoon.

(2) In the F1 region, the behavior of the electron density was similar to that in the E region with the additional phenomenon that the ledge in the true height profile either disappeared or was diminished at all stations during the middle of the eclipse. This effect was less noticeable at Anchorage where the eclipse occurred in the morning and where consequently the normal behavior in the absence of an eclipse would have been for the ledge to become more pronounced.

(3) In the F2 region close solar control of the electron density existed only for a brief period following first contact. Thereafter, changes in the electron density distribution were determined by the competitive effects of transport, production, and recombination. The contours of constant plasma frequency indicate a transition level at approximately 200 to 230 km above which transport processes appeared to be dominant over recombination.

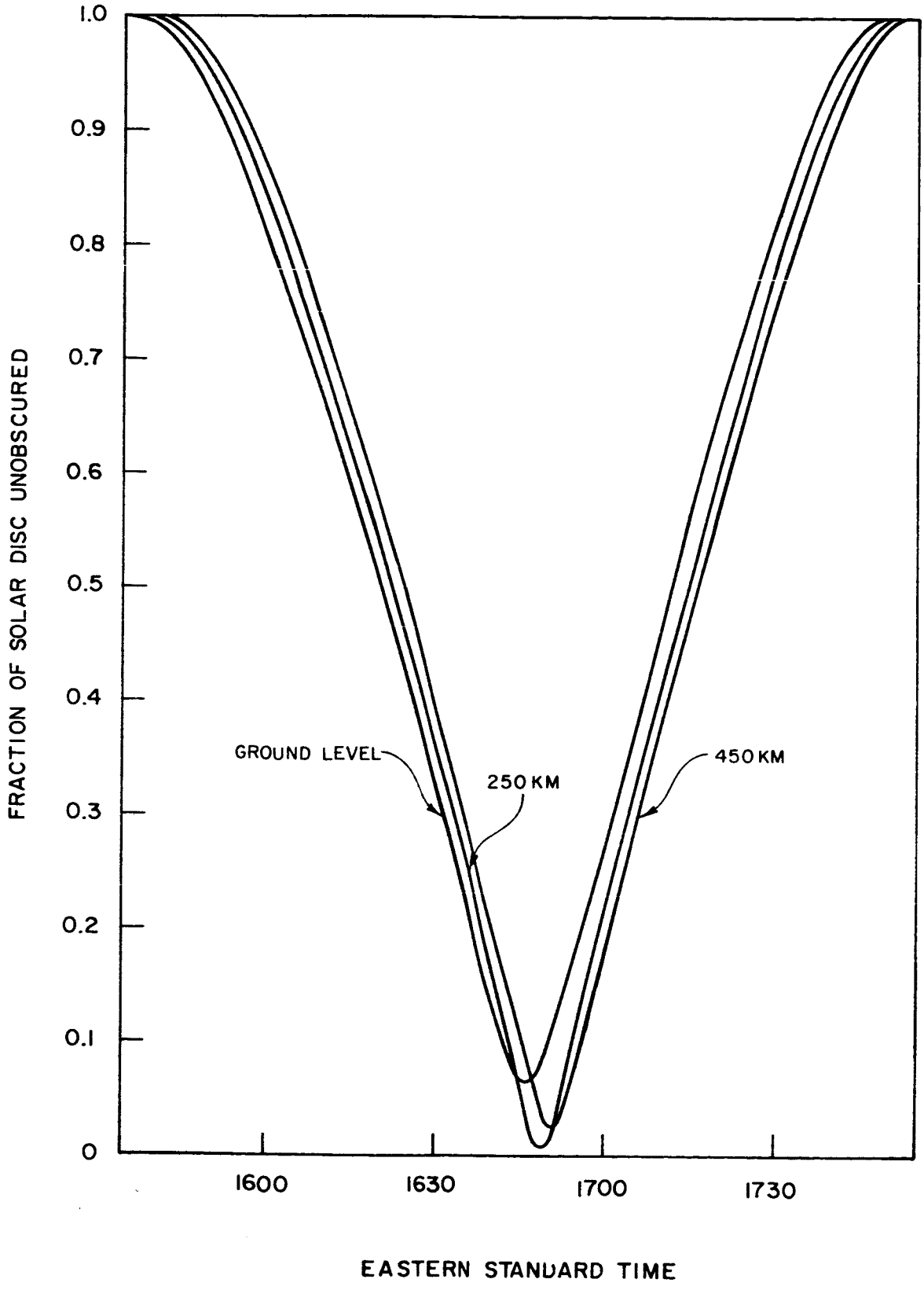

Figure 1. Fraction of Solar Disc Unobscured vs. Time at Millstone Hill (Westford), Massachusetts. The eclipse was total at 300 km at 1650 EST.

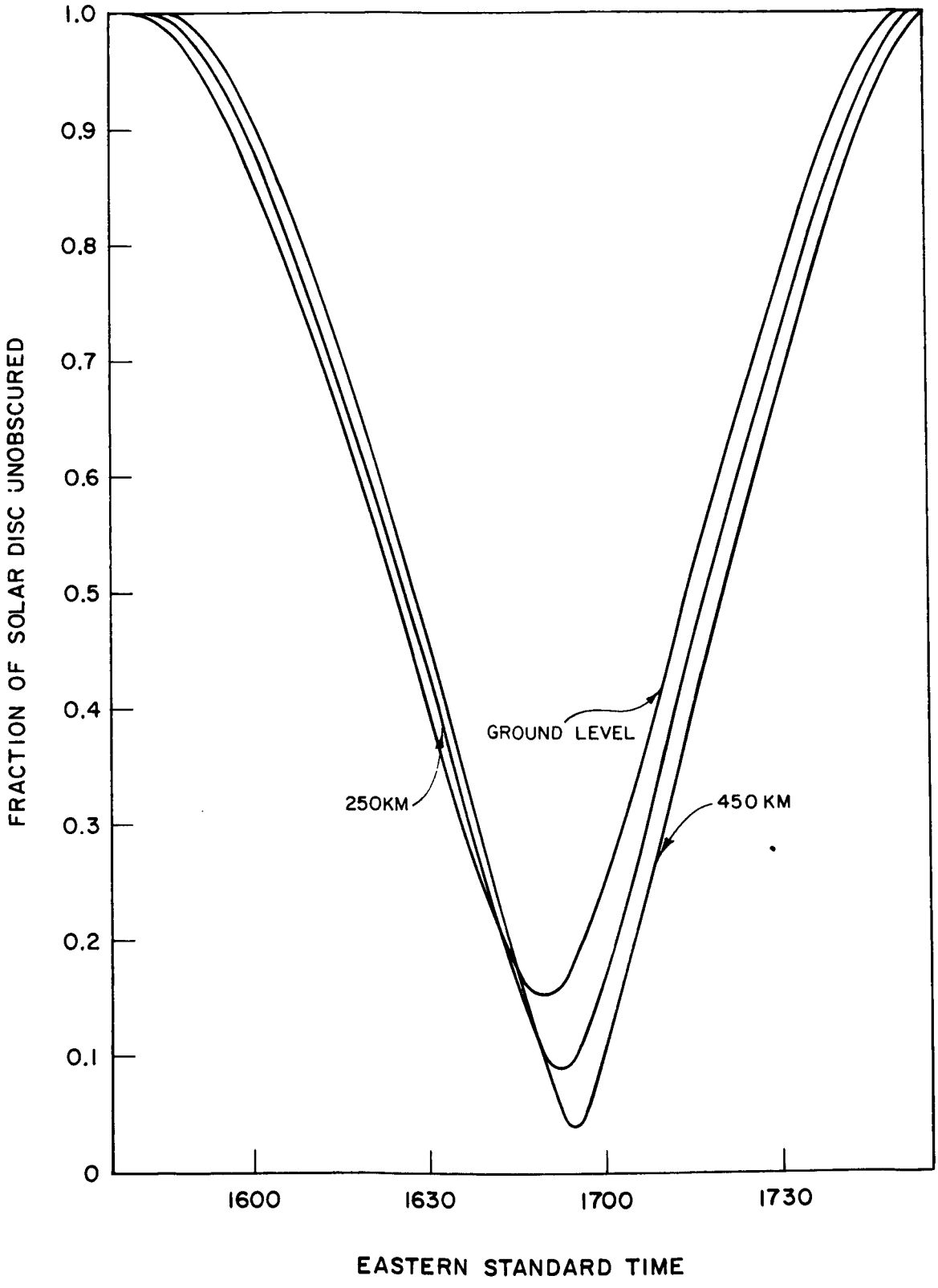

Figure 2. Fraction of Solar Disc Unobscured vs. Time at Fort Monmouth, New Jersey.

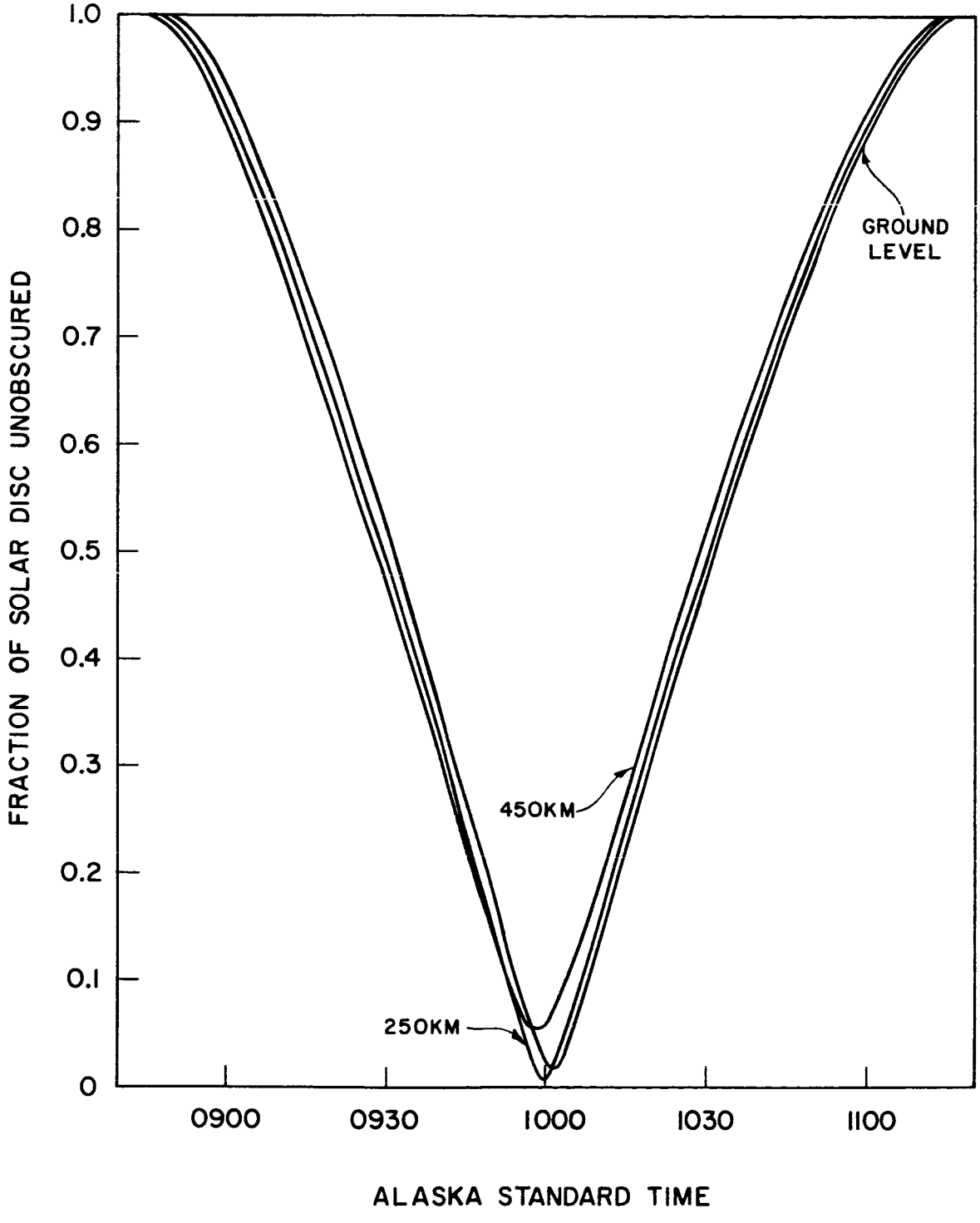

Figure 3. Fraction of Solar Disc Unobscured vs. Time at Anchorage, Alaska. The eclipse was total at heights of 150-200 km at 1000 AST.

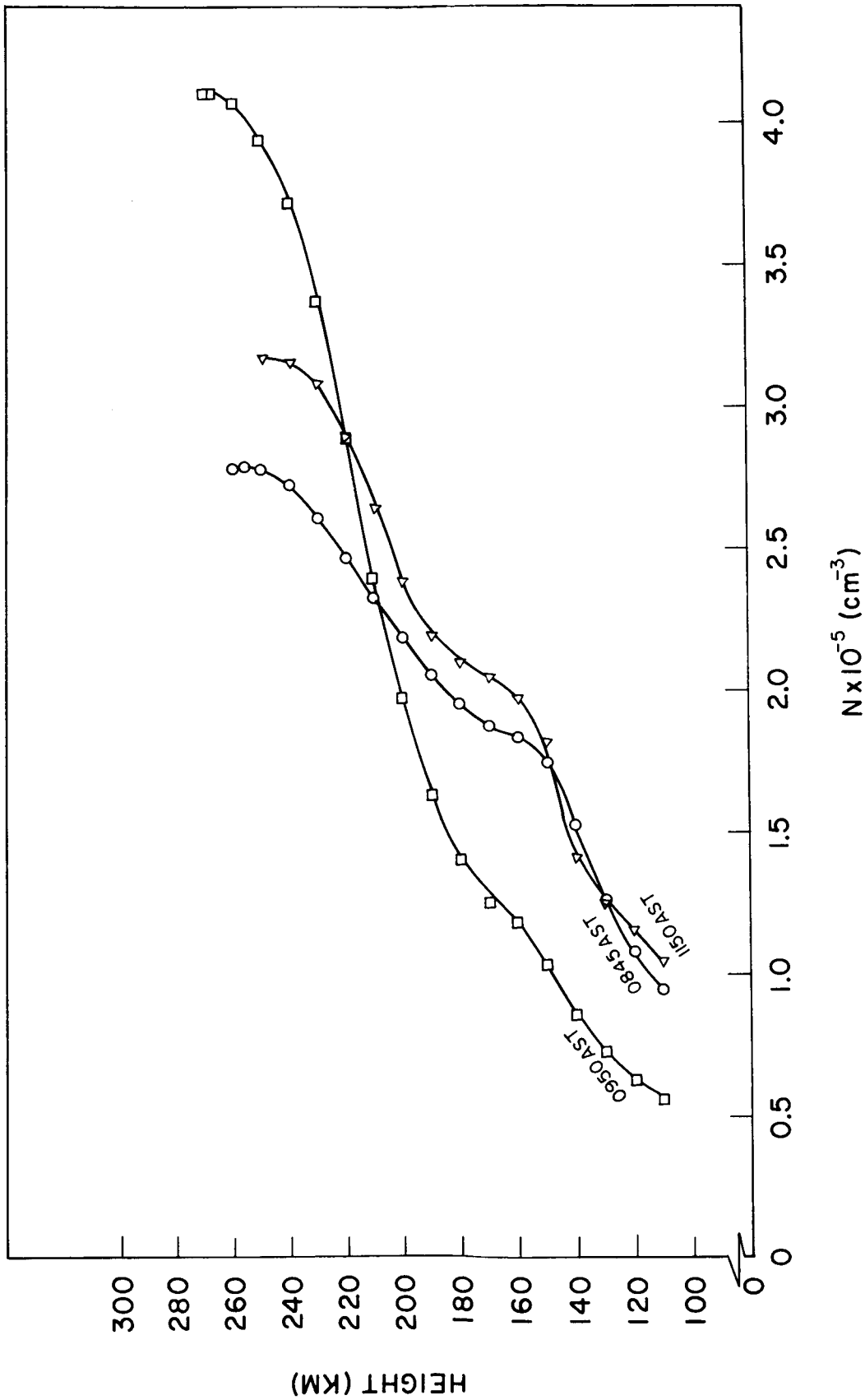

Figure 4. Electron Density vs. True Height at Anchorage, Alaska.

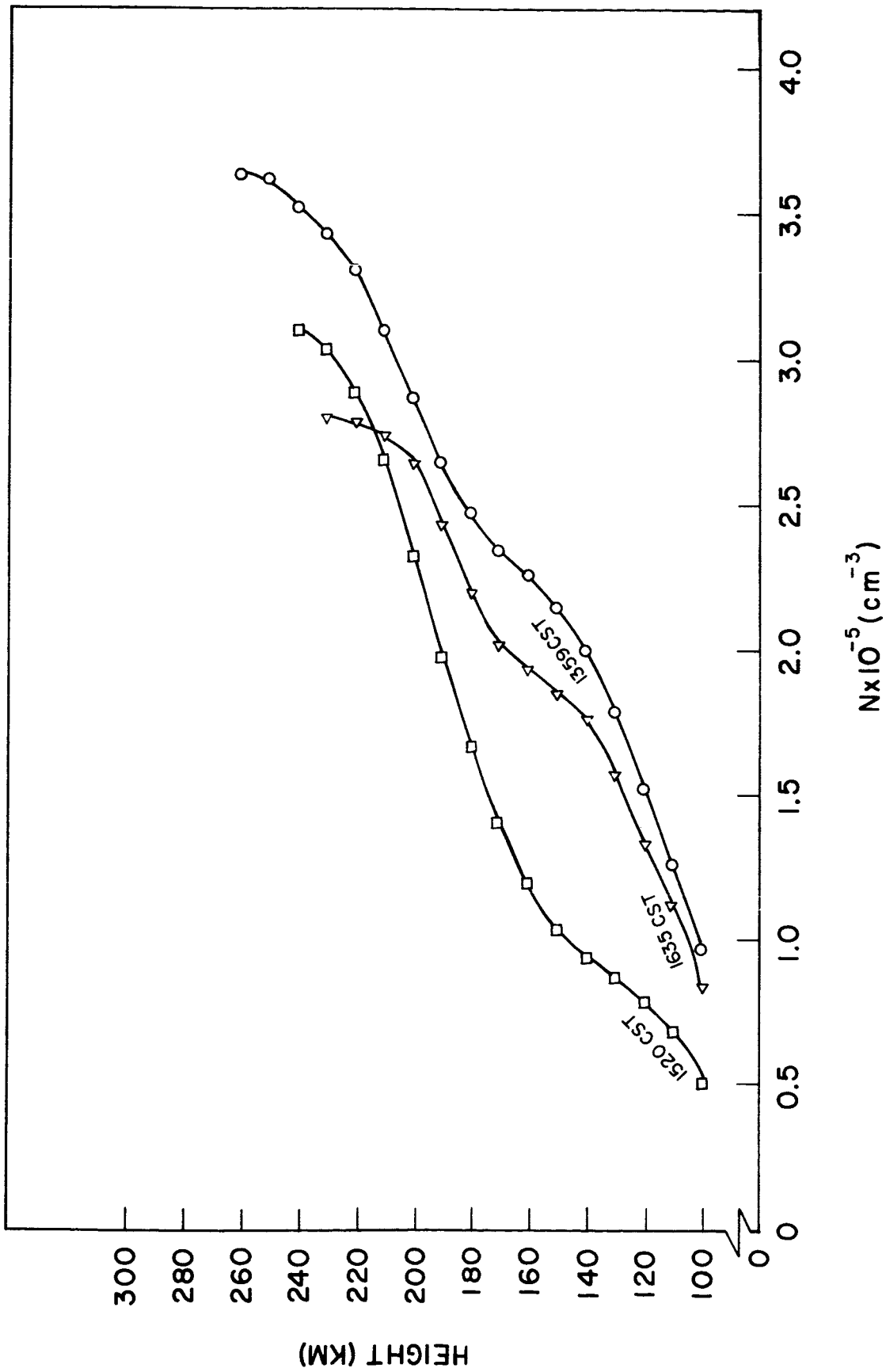

Figure 5. Electron Density vs. True Height at Fort Churchill, Manitoba.

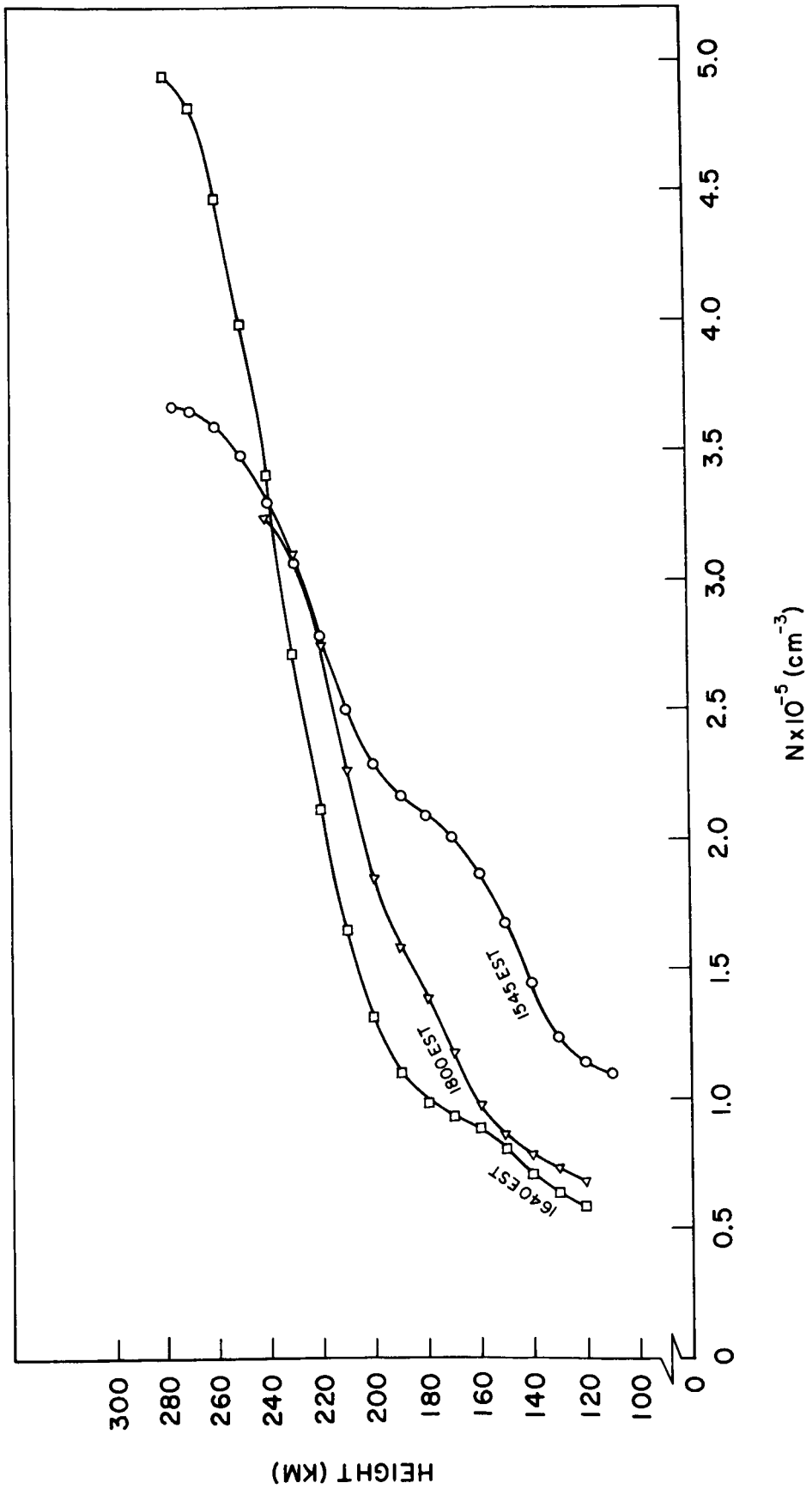

Figure 6. Electron Density vs. True Height at Fort Monmouth, New Jersey.

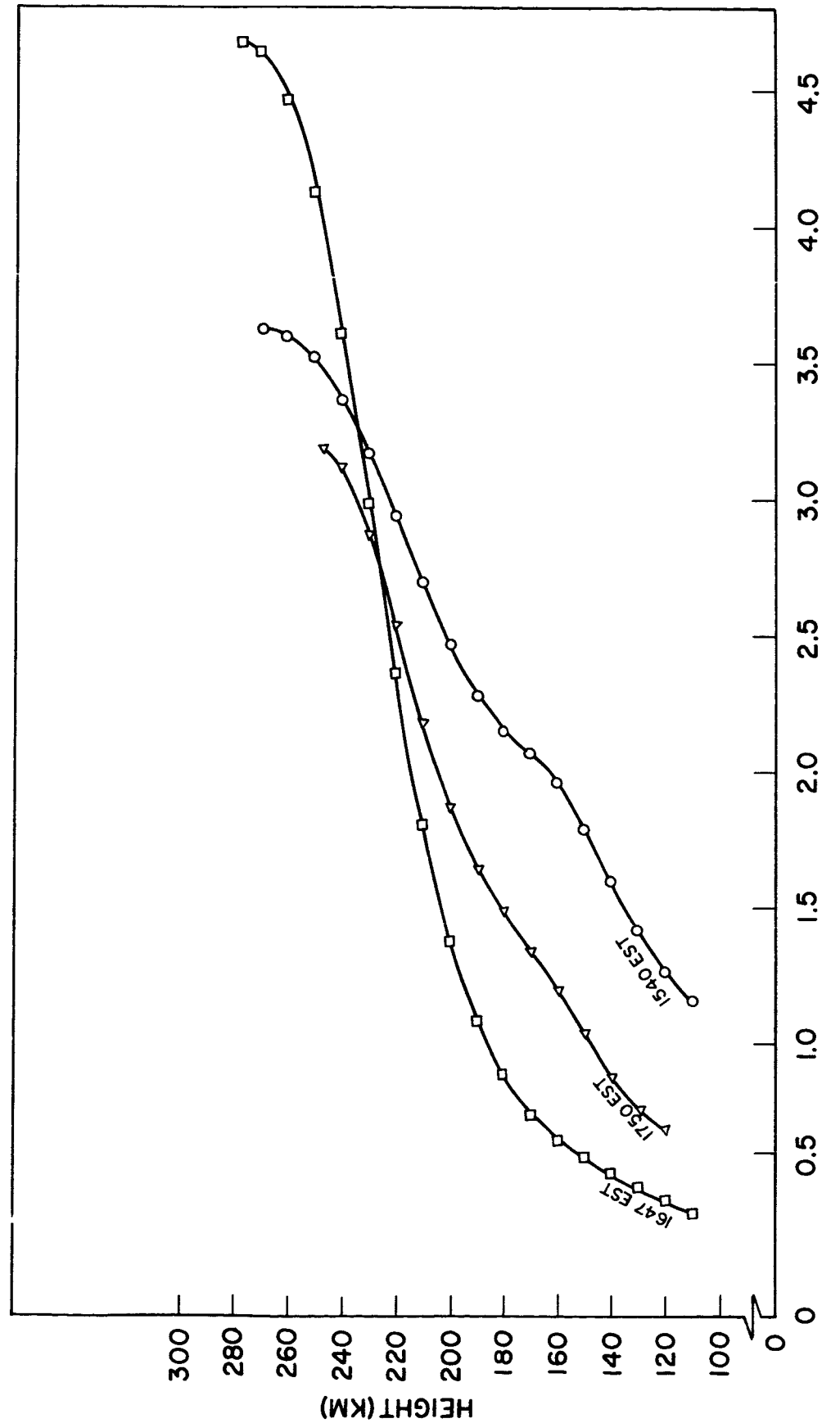

Figure 7. Electron Density vs. True Height at Millstone Hill (Westford), Massachusetts.

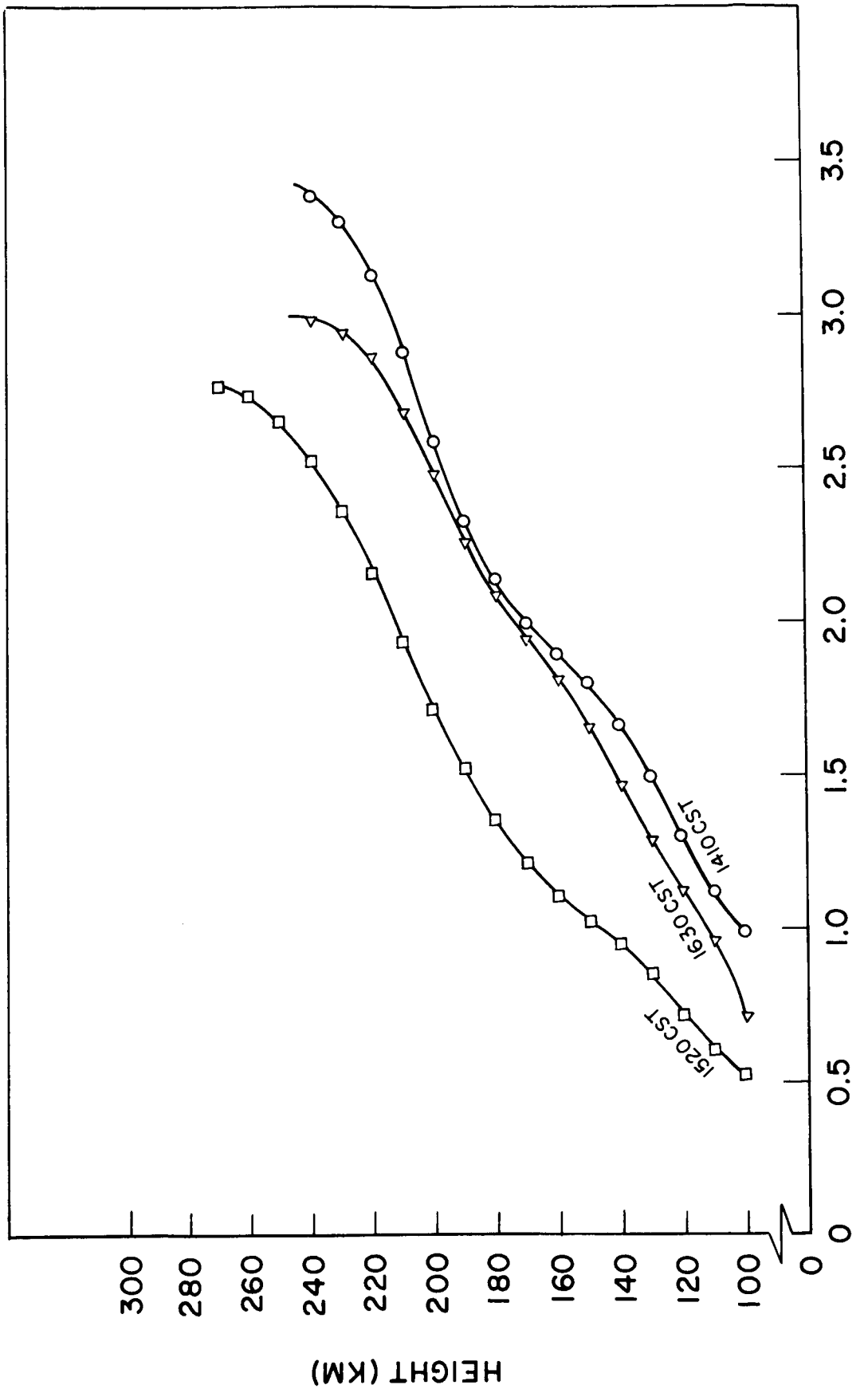

Figure 8. Electron Density vs. True Height at Winnipeg, Manitoba.

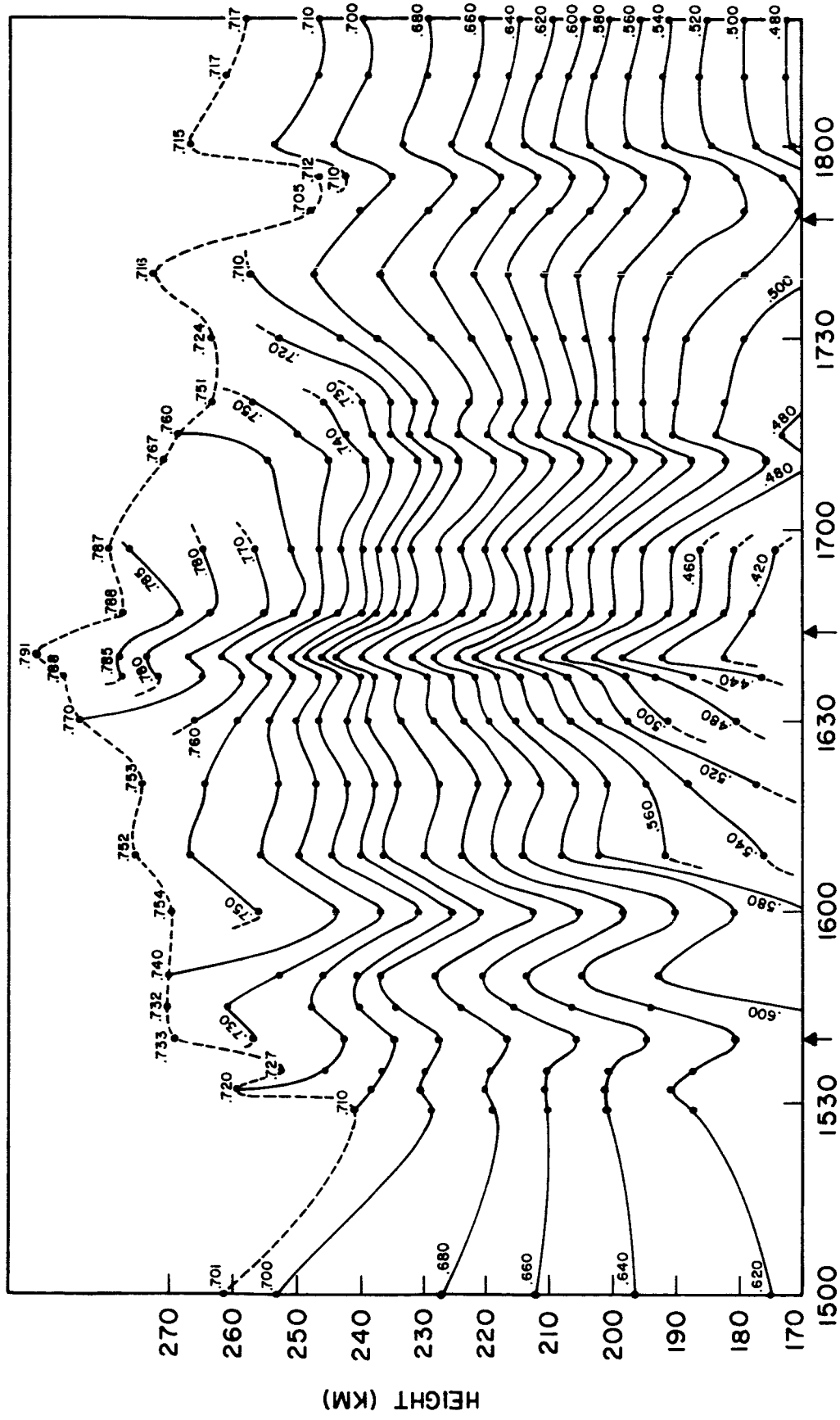

Figure 9. Contours of Constant Plasma Frequency at Millstone Hill (Westford), Massachusetts. The arrows on the time scale indicate times of first contact, maximum phase, and fourth contact at ground level.

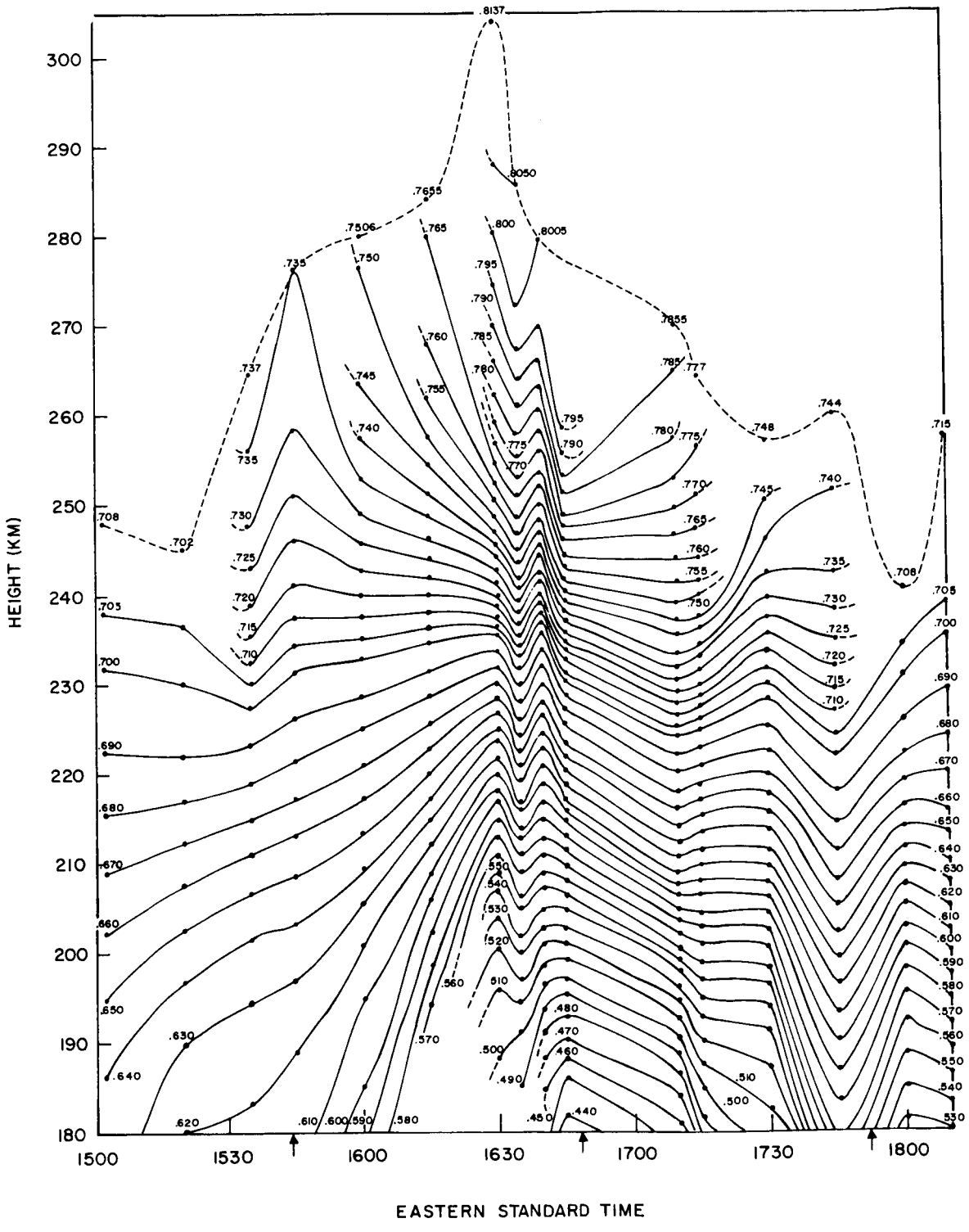

Figure 10. Contours of Constant Plasma Frequency at Fort Monmouth, New Jersey.

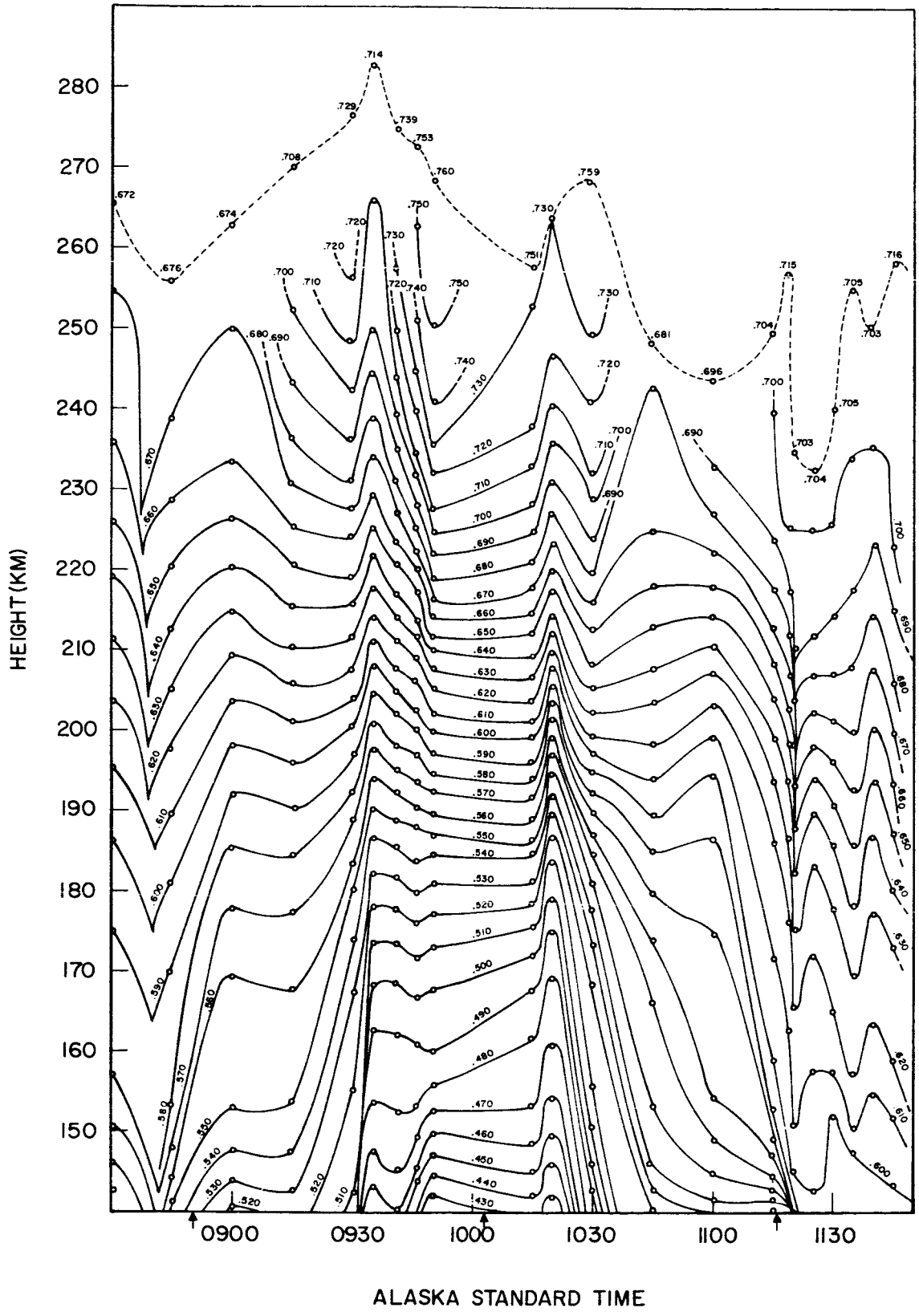

Figure 11. Contours of Constant Plasma Frequency at Anchorage, Alaska. Contours are indicated by log f_N (MHz). Dotted line is $h_m F2$ and log $f_o F2$ is indicated at points.

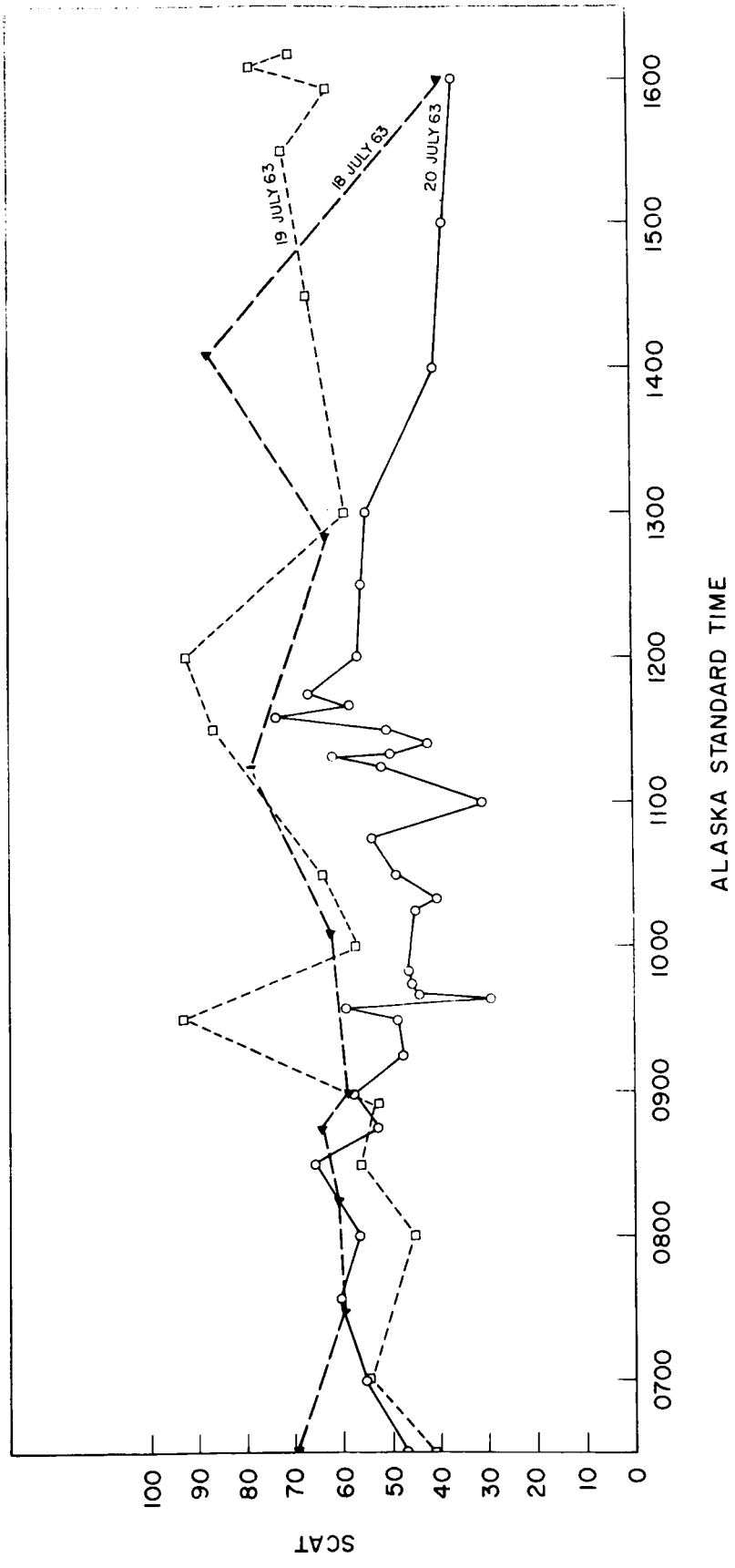

Figure 12. Scat vs. Time at Anchorage, Alaska, 18-20 July 1963. S_{cat} is in kilometers.

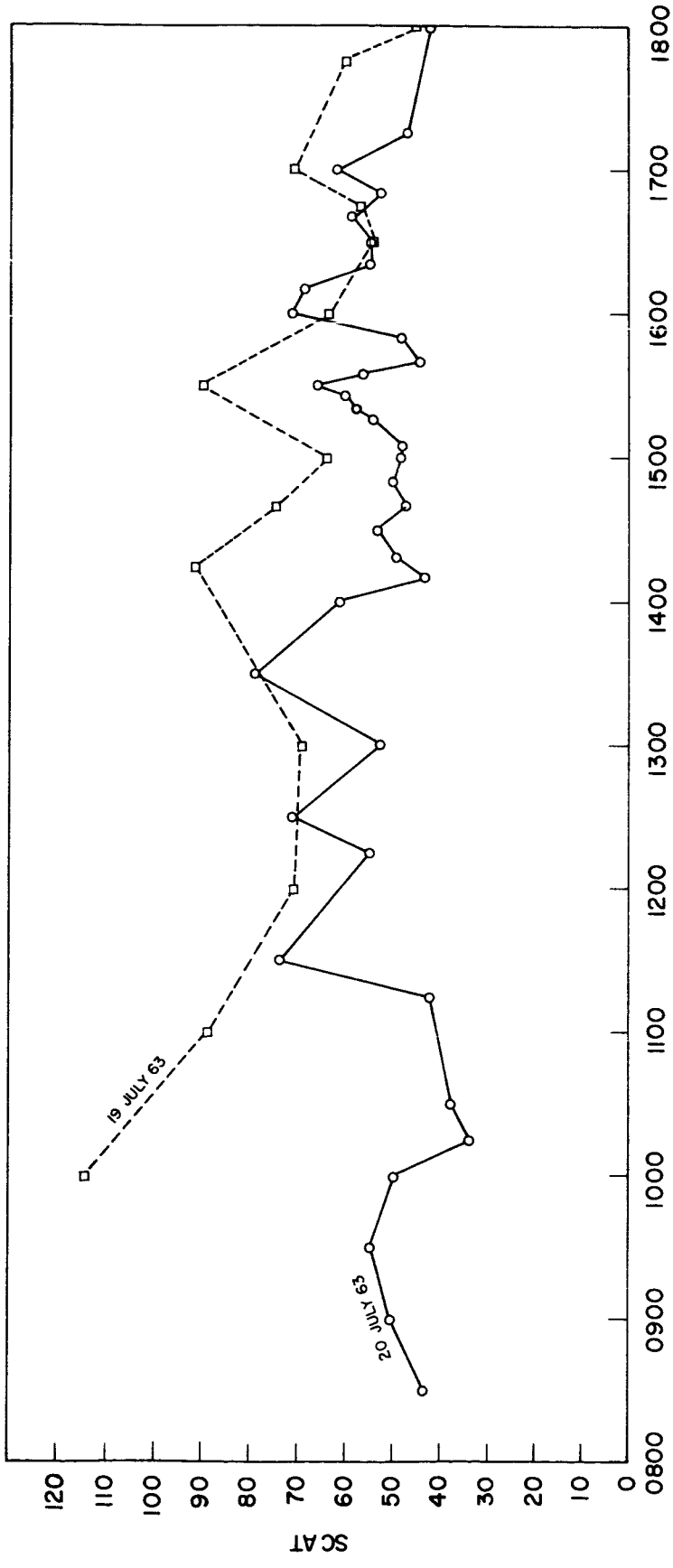

Figure 13. S_{cat} vs. Time at Fort Churchill, Manitoba, 19-20 July 1963.

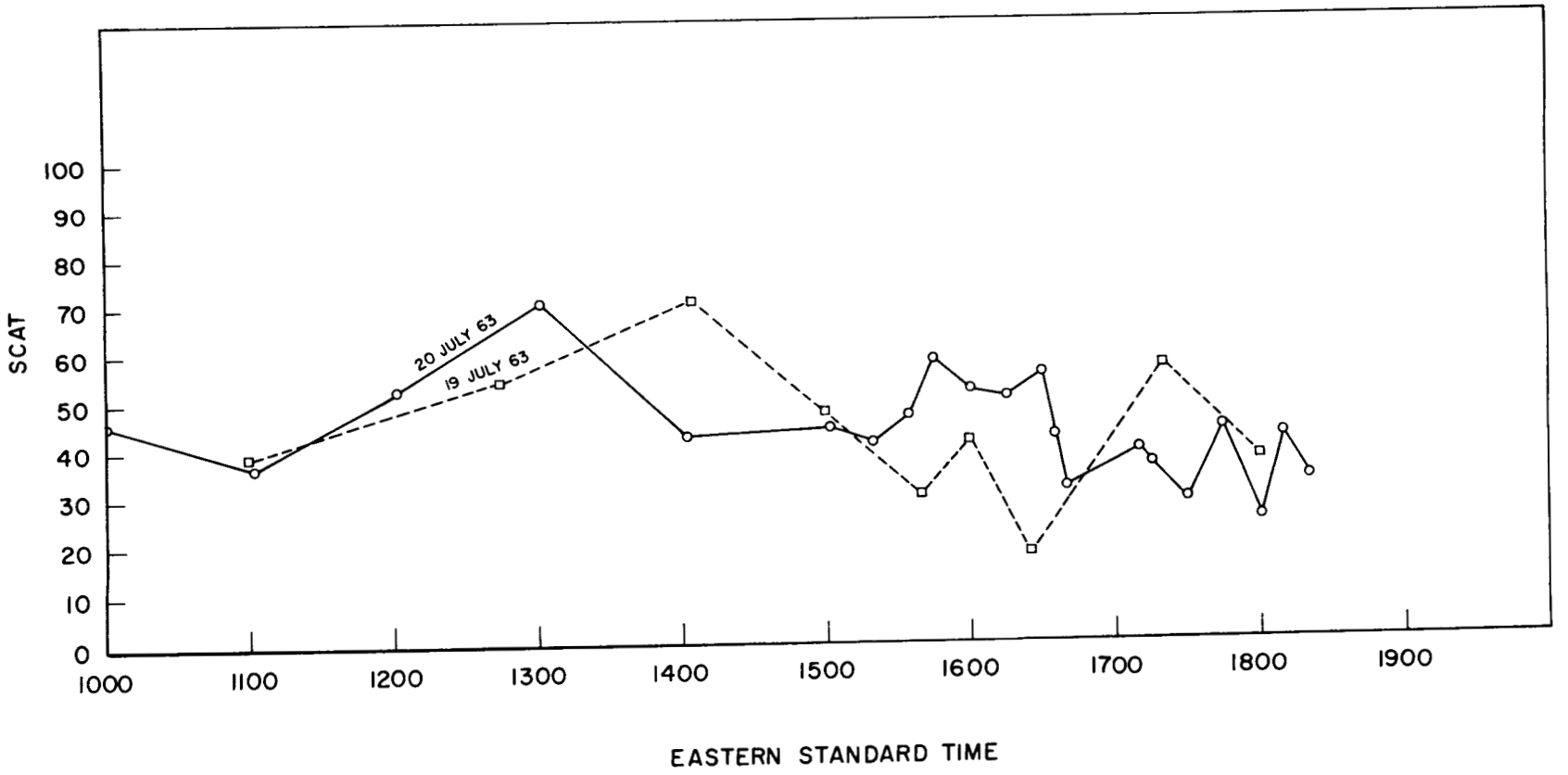

Figure 14. S_{cat} vs. Time at Fort Monmouth, New Jersey, 19-20 July 1963.

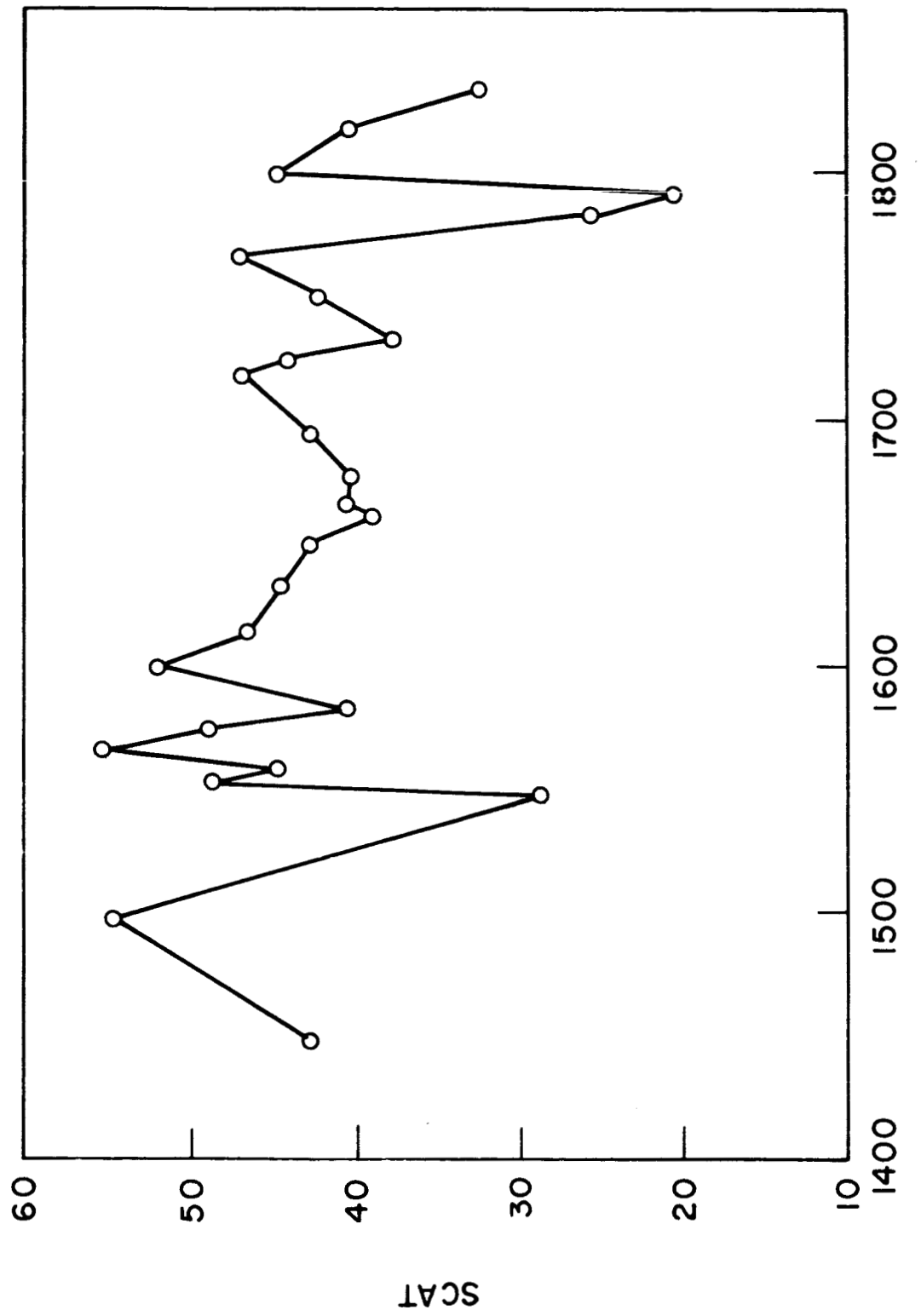

Figure 15. Scat vs. Time at Millstone Hill (Westford), Massachusetts, 20 July 1963.

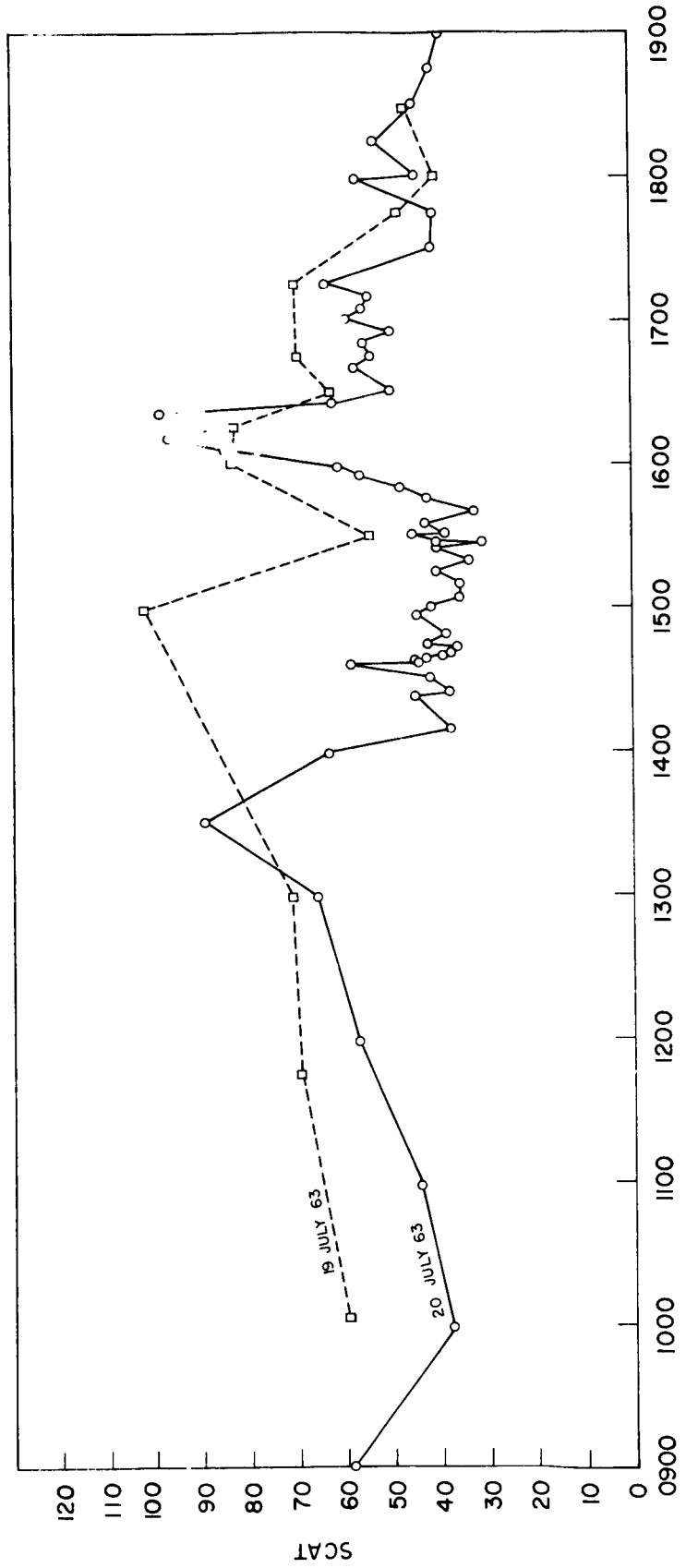

Figure 16. Scat vs. Time at Winnipeg, Manitoba, 19-20 July 1963.

References

Bowhill, S. A., The effective recombination coefficient of an atmosphere containing a mixture of ions, J. Atmos. Terr. Phys., 20, 19 (1961).

Dalgarno, A., et al., Electron temperatures in the ionosphere, Planet. Space Sci., 11, 463 (1963).

Evans, J. V., The effects of the 20 July 1963 solar eclipse on the F-region of the ionosphere, in Proc. of AFCRL Workship on 20 July 1963 Solar Eclipse, Air Force Cambridge Res. Lab., AFCRL-64-962, 1964.

Evans, J. V., An F-region eclipse, J. Geophys. Res., 70, 131, (1965a).

Evans, J. V., On the behavior of f_oF2 during solar eclipses, J. Geophys. Res., 70, 733 (1965b).

Friedman, H., The sun's ionizing radiations, in Physics of the Upper Atmosphere, ed. by J. A. Ratcliffe, New York and London: Academic Press, 1960.

Geisler, J. E., and S. A. Bowhill, An Investigation of Ionosphere-Protonosphere Coupling, Aeronomy Rep. No. 5, Aeronomy Lab., University of Illinois.

Gledhill, J. A., The effects of a solar eclipse on a stratified atmosphere, J. Atmos. Terr. Phys., 16, 360 (1959).

Hanson, W. B., Electron temperatures in the upper atmosphere, in Space Research III, ed. by W. Priester, Amsterdam: North Holland Publishing Co., 1963.

Hirono, M., Effect of gravity and ionization pressure gradient on the vertical drift in the F2 region, Rept. Ionos. Res. Japan, 9, 95 (1955).

Hirsh, A. J., The electron density distribution in the F region of the ionosphere, J. Atmos. Terr. Phys., 17, 86 (1959).

Hirsh, A. J., The electron density distribution in the F region of the ionosphere, in Electron Density Profiles in the Ionosphere and Exosphere, ed. by B. Maehlum, London: Pergamon Press, 1962.

Ilias, D., and M. Anastassiadis, Distribution of the electron density in the ionosphere over Athens during the solar eclipse of 15 February 1961, in Electron Density Profiles in the Ionosphere and Exosphere, ed. by B. Maehlum, London: Pergamon Press, 1962.

Miner, R. J., "L" band solar flux measurements during partial eclipse of 20 July 1963, in Proc. of AFCRL Workshop on 20 July 1963 Solar Eclipse, Air Force Cambridge Research Lab., AFCRL-64-962, 1964.

Minnis, C. M., The effective recombination coefficients in the E and F1 layers, in Solar Eclipses and the Ionosphere, Spec. Suppl. to J. Atmos. Terr. Phys., 6 (1956).

Nicolet, M., Recombination in the F2 layer, in Electron Density Profiles in the Ionosphere and Exosphere, ed. by B. Maehlum, London: Pergamon Press, 1962.

Paul, A. K., and J. W. Wright, Some results of a new method for obtaining ionospheric N(h) profiles with a bearing on the structure of the lower F-region, in Electron Density Distribution in the Ionosphere and Exosphere, ed. by E. Thrane, Amsterdam: North Holland Publishing Co., 1964.

Pound, T. R., Faraday rotation and vertical sounding observations of the ionosphere during July 20, 1963 solar eclipse, in Proc. of AFCRL Workshop on 20 July 1963 Solar Eclipse, Air Force Cambridge Research Lab., AFCRL-64-962, 1964.

Pound, T. R., and K. C. Yeh, Response of the Ionosphere to a Change of Electron Temperature, presented at 1965 Fall URSI Meeting, Dartmouth College, October, 1965.

Pound, T. R., et al., Ionospheric electron content during July 20, 1963 solar eclipse, J. Geophys. Res., 71, 326 (1966).

Ratcliffe, J. A., A survey of solar eclipses and the ionosphere, in Solar Eclipses and the Ionosphere, Spec. Suppl. to J. Atmos. Terr. Phys., 6 (1956a).

Ratcliffe, J. A., The formation of the ionospheric layers F1 and F2, J. Atmos. Terr. Phys., 8, 260 (1956b).

Risbeth, H., Guide to the theory of the quiet F layer, in Electron Density Profiles in the Ionosphere and Exosphere, ed. by B. Maehlum, London: Pergamon Press, 1962.

Smith, L. G., et al., Rocket measurements of the ionosphere during the eclipse of July 20, 1963, in Proc. of AFCRL Workshop on 20 July 1963 Solar Eclipse, Air Force Cambridge Research Lab., AFCRL-64-962, 1964.

Szendrei, M. E., and M. W. McElhinny, The behaviour of the E1 layer during the solar eclipse of 25 December 1954, in Solar Eclipses and the Ionosphere, Spec. Suppl. to J. Atmos. Terr. Phys., 6 (1956).

Wright, J. W., Mean Electron Density Variation of the Quiet Ionosphere, NBS Tech. Note 40-13, 1962.

Wright, J. W., On the implication of diurnal, seasonal, and geographical variations in composition of the high atmosphere, from F-region measurements, in Electron Density Distribution in the Ionosphere and Exosphere, ed. by E. Thrane, Amsterdam: North Holland Publishing Co., 1964.